MgATP-Bound and Nucleotide-Free Structures of a Nitrogenase Protein Complex between the Leu 127Δ-Fe-Protein and the MoFe-Protein[†,‡]

Hsiu-Ju Chiu,[§,||] John W. Peters,[§,⊥] William N. Lanzilotta,[#] Matthew J. Ryle,[#] Lance C. Seefeldt,[#] James B. Howard,[@] and Douglas C. Rees*[,§,||]

Division of Chemistry and Chemical Engineering, Mail Code 147-75CH, California Institute of Technology, Pasadena, California 91125, Department of Chemistry and Biochemistry, Utah State University, Logan, Utah 84322, Department of Biochemistry, University of Minnesota, Minneapolis, Minnesota 55455, and Howard Hughes Medical Institute, California Institute of Technology, Pasadena, California 91125

Received July 14, 2000; Revised Manuscript Received November 7, 2000

ABSTRACT: A mutant form of the nitrogenase iron protein with a deletion of residue Leu 127, located in the switch II region of the nucleotide binding site, forms a tight, inactive complex with the nitrogenase molybdenum iron (MoFe) protein in the absence of nucleotide. The structure of this complex generated with proteins from *Azotobacter vinelandii* (designated the L127Δ-Av2−Av1 complex) has been crystallographically determined in the absence of nucleotide at 2.2 Å resolution and with bound MgATP (introduced by soaking) at 3.0 Å resolution. As observed in the structure of the complex between the wild-type *A. vinelandii* nitrogenase proteins stabilized with ADP·AlF_4^-, the most significant conformational changes in the L127Δ complex occur in the Fe-protein component. While the interactions at the interface between the MoFe-protein and Fe-proteins are conserved in the two complexes, significant differences are evident at the subunit−subunit interface of the dimeric Fe-proteins, with the L127Δ-Av2 structure having a more open conformation than the wild-type Av2 in the complex stabilized by ADP·AlF_4^-. Addition of MgATP to the L127Δ-Av2−Av1 complex results in a further increase in the separation between Fe-protein subunits so that the structure more closely resembles that of the wild-type, nucleotide-free, uncomplexed Fe-protein, rather than the Fe-protein conformation in the ADP·AlF_4^- complex. The L127Δ mutation precludes key interactions between the Fe-protein and nucleotide, especially, but not exclusively, in the region corresponding to the switch II region of G-proteins, where the deletion constrains Gly 128 and Asp 129 from forming hydrogen bonds to the γ-phosphate and activating water for attack on this group, respectively. These alterations account for the inability of this mutant to support mechanistically productive ATP hydrolysis. The ability of the L127Δ-Av2−Av1 complex to bind MgATP demonstrates that dissociation of the nitrogenase complex is not required for nucleotide binding.

Central to understanding substrate reduction by nitrogenase is the elucidation of the process by which ATP hydrolysis is coupled to electron transfer (for reviews, see refs *1*−*5*). From the initial sequence and structural characterization of the Fe-protein component, it was evident that this nucleotide-binding, redox-active component of the nitrogenase complex could have functional similarities to the G-protein family of signal transduction proteins. Not only does the Fe-protein structure have the general folding pattern of the G-protein family (reviewed in refs *6* and *7*), but it also contains many of the shorter sequences and structural motifs involved in nucleotide binding such as the Walker P-loop, the Mg−phosphate binding region, and the so-called switch II region which, in the case of the Fe-protein, includes two of the four ligands to the [4Fe-4S] cluster, the electron transfer center. Not withstanding the substantial structural similarities to the G-protein family, the Fe-protein has a significant functional difference; namely, in contrast to members of the G-protein family which have a basal rate of nucleotide hydrolysis, the Fe-protein apparently is capable of catalytic nucleotide hydrolysis only when in complex with the second nitrogenase component, the MoFe-protein [although the Fe-protein has recently been reported to slowly hydrolyze ATP in the absence of the MoFe-protein (*8*)]. It is in the transient complex between the Fe-protein and the MoFe-protein that electron transfer occurs, ultimately resulting in substrate reduction at a remote site (FeMo-cofactor) in the MoFe-protein. Hence, we have speculated that nucleotide hydrolysis

[†] This work was supported by NIH Grant GM45162 (D.C.R. and J.B.H.), NSF Grant MCB 9722937 (L.C.S.), and NIH Postdoctoral Fellowship GM18142 (J.W.P.). The rotation camera facility at the Stanford Synchrotron Radiation Laboratory is supported by the Department of Energy Office of Basic Sciences and the NIH Biomedical Technology Program, Division of Research Resources.

[‡] The coordinates for these structures have been deposited in the RCSB Protein Data Bank for release upon publication (entries 1G20 and 1G21 for the structures of the L127Δ-Av2−Av1 nitrogenase complex in the absence and presence of ATP, respectively).

* To whom correspondence should be addressed. Telephone: (626) 395-8393. Fax: (626) 744-9524. E-mail: dcrees@caltech.edu.

[§] Division of Chemistry and Chemical Engineering, California Institute of Technology.

[||] Howard Hughes Medical Institute; California Institute of Technology.

[⊥] Present address: Department of Chemistry and Biochemistry, Utah State University, Logan, UT 84322.

[#] Utah State University.

[@] University of Minnesota.

10.1021/bi001645e CCC: $20.00
Published on Web 12/21/2000

may serve as a regulator of conformational switching leading to electron transfer (*1*, *9*, *10*).

Although some of these ideas about the mechanism of nitrogenase originated from inspection of the individual protein structures, the structure determination of the complex between the *Azotobacter vinelandii* nitrogenase MoFe-protein and the Fe-protein (abbreviated Av1 and Av2, respectively) stabilized by the nucleotide analogue ADP·AlF_4^- directly addressed many of these issues (*9*). Aluminum fluoride serves as a transition state analogue for the γ-phosphate during nucleotide hydrolysis, and has been extensively exploited in studies of G-proteins and other nucleotide-dependent proteins (*11*). In this complex, Av2 undergoes a large conformational change relative to its structure in the nucleotide-free, autonomous state in the absence of Av1. In the complex, the two chemically identical subunits of Av2, bridged by the [4Fe-4S] cluster, rotate ~13° toward each other, leading to new interactions across the interface between the Av2 subunits in the vicinity of the two bound nucleotides. Most notably, residues Asp 129 and Lys 10 become positioned to stabilize the attacking water and the departing phosphate, respectively, in the putative transition state. In contrast, there are only small locally confined conformational changes in Av1. The conformational change in Av2 results in a modified binding site with a higher degree of complementation to the Av1 binding surface that permits the Av2 [4Fe-4S] cluster (the electron donor) to approach the Av1 P-cluster (which serves as the initial electron acceptor from the Fe-protein) ~4 Å closer than possible with simple van der Waals contact between the individual protein components.

Several years ago, an altered Av2 was constructed by deletion of Leu 127 (denoted L127Δ-Av2) (*12*, *13*). Leu 127 is located in the conserved sequence motif Asp 125-X_2-X_3-Gly 128 that is part of the switch II region and is involved in Mg−γ-phosphate binding (*14*). This region undergoes significant peptide backbone conformational changes in the Av2−ADP·AlF_4^-−Av1 complex, including the formation of an amide hydrogen bond from Gly 128 to the AlF_4^- (which would be equivalent to a hydrogen bond to an oxygen of the γ-phosphate of ATP) and the stabilization by Asp 129 of the attacking water. L127Δ-Av2 was reported to have some physicochemical properties similar to those of states of native Av2 with bound nucleotide (*12*, *13*). Intriguingly, this altered protein formed a tight complex with Av1 in the absence of bound nucleotide. Although reduction of substrates does not occur in this complex (*12*), one-electron transfer from the $[4Fe\text{-}4S]^+$ form of the Fe-protein to the two-electron-oxidized state of the P-cluster (P^{OX}) in the MoFe-protein has been observed (*13*, *15*). Nucleotides can bind to the L127Δ-Av2−Av1 complex, and low levels of ATP hydrolysis have been detected.[1]

These properties suggested that the structure of the complex when compared to the wild-type Av2−ADP·AlF_4^-−Av1 complex might lead to a better understanding of the various stages in complex formation, the relative importance of some of the conformational changes, and events leading to nucleotide hydrolysis. In this paper, we report the structures of the L127Δ-Av2−Av1 complex and the Mg-ATP bound L127Δ-Av2−ATP−Av1 complex as determined by X-ray crystallography. These new structures are correlated to that of the ADP·AlF_4^--stabilized complex of wild-type proteins. The binding regions between Av1 and Av2 in all three complexes are notably similar, if not essentially identical, including the close approximation of the electron transfer centers. Nevertheless, our results clearly show that the conformational changes involving the inter-Av2 subunit contacts and those in the switch II region seen in the ADP·AlF_4^--stabilized complex are altered or missing in the complex with L127Δ-Av2. Therefore, these contacts are likely required for mechanistically competent nucleotide hydrolysis. Surprisingly, the addition of ATP to the complex alters the L127Δ-Av2 structure so that it looks less like the Av2−ADP·AlF_4^- structure rather than more like it, illustrating the complexities of the interactions between nitrogenase proteins and nucleotides, and their sensitivities to mutagenesis.

Table 1: Data and Refinement Statistics

	L127Δ-Av2−Av1	L127Δ-Av2−ATP−Av1
Data Statistics		
space group	*C*2	$P2_12_12_1$
a (Å)	264.2	110.5
b (Å)	111.5	121.5
c (Å)	121.6	264.9
β (deg)	97.4	90.0
resolution range (Å)	20.0−2.2	20.0−3.0
no. of observations	1092580	386858
no. of unique reflections	167675	52828
R_{merge} (%)[a,b]	11.2 (29.6)	13.2 (28.2)
completeness (%)[a]	94.7 (83.2)	73.5 (28.7)
Refinement Statistics		
resolution range (Å)	20.0−2.2	20.0−3.0
R	0.219	0.238
R-free[c]	0.255	0.285
rmsds		
bond lengths (Å)	0.009	0.011
bond angles (deg)	1.83	1.79
Ramachandran (%)[d]		
most favored	89.5	88.8
additional allowed	10.1	10.8
generally allowed	0.3	0.4
disallowed	0.1	0.0
average *B*-factor (Å^2)		
main chain	37.2	30.2
side chain	38.9	32.1
metalloclusters	28.1	28.4
solvent	36.2	−
ATP	−	63.5

[a] Values in parentheses correspond to the highest-resolution shell (2.24−2.2 Å for L127Δ-Av2−Av1 and 3.11−3.00 Å for L127Δ-Av2−ATP−Av1). [b] $R_{merge} = \Sigma_{hkl,I}[\Sigma_I(|I_{hkl,I} - \langle I_{hkl}\rangle|)]/\Sigma_{hkl,I}\langle I_{hkl}\rangle$, where I_{hkl} is the intensity of an individual measurement of the reflection with indices *hkl* and $\langle I_{hkl}\rangle$ is the mean intensity of that reflection. [c] *R*-free is defined for 5% of the data omitted from the refinement. [d] The most favored, additional, generally allowed, and disallowed regions are defined by PROCHECK (*40*).

EXPERIMENTAL PROCEDURES AND STRUCTURE DETERMINATION

The methods for construction of the mutant L127Δ-Av2 strain by oligonucleotide-directed mutagensis and for isolation of the L127Δ-Av2 protein have been described previously (*16*). Av1 was isolated as described in ref *17*. The L127Δ-Av2−Av1 complex was formed by incubation of a

[1] M. J. Ryle and L. C. Seefeldt, unpublished results.

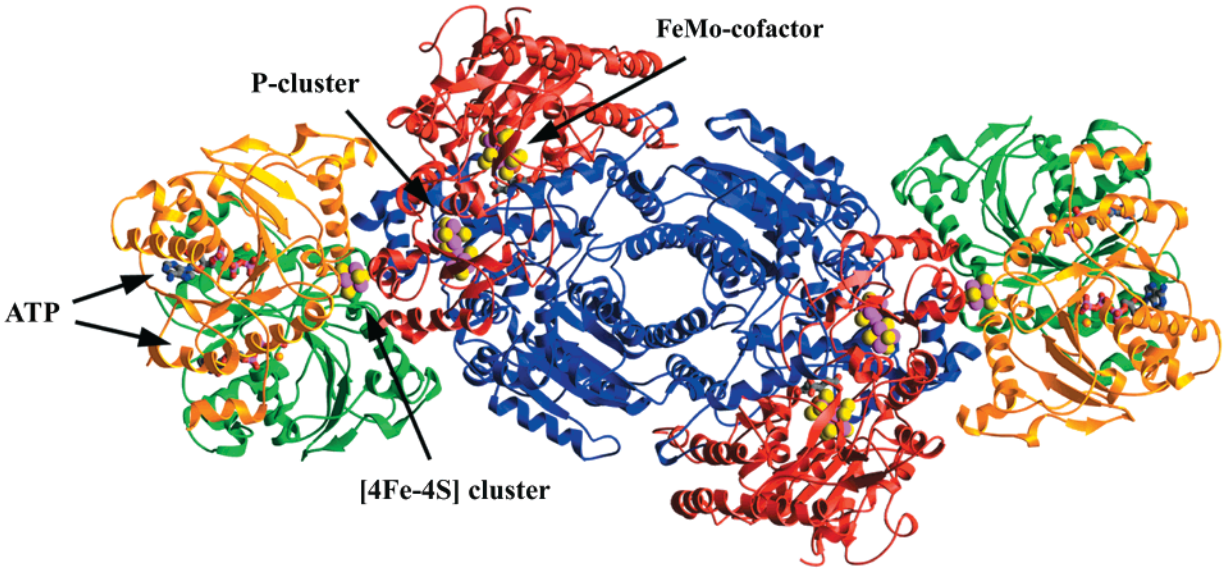

FIGURE 1: Ribbons diagram of the L127Δ-Av2−ATP−Av1 complex, viewed down the 2-fold axis that relates each αβ dimer of Av1 and the associated L127Δ-Av2 dimer. This orientation is also approximately perpendicular to the 2-fold axis that relates the Fe-protein subunits in each dimer. The MoFe-protein α-subunits are in red; the β-subunits are in blue, and the individual subunits of each Fe-protein are in gold and green. The cofactors are shown in space-filling representations, and the MgATP molecules are in ball-and-stick representations. Atoms are color-coded with Mg in gold, Mo in orange, Fe and P in magenta, S in yellow, O in red, N in blue, and C in gray. Molecular figures in this paper were prepared with Ribbons (*41*), Molscript (*42*), and Raster3D (*43*).

mixture of L127Δ-Av2 and Av1 (4:1 molar ratio) at a final protein concentration of ∼50 mg/mL for approximately 1 h. The L127Δ-Av2−Av1 complex was separated from excess L127Δ-Av2 by chromatography on a Sephacyl-200 column. Individual fractions from the gel filtration chromatography were evaluated for purity and for content by SDS−polyacrylamide gel electrophoresis. The purification of all native and altered protein components was performed under anaerobic conditions in the presence of 1 mM sodium dithionite.

The L127Δ-Av2−Av1 complex was crystallized by the microcapillary batch diffusion method (*18*) using 30% PEG 4000 as the precipitating agent in 0.2 M NaOAc, 0.1 M Tris (pH 8.5) buffer containing 1 mM sodium dithionite. The brown crystals grew in 1−2 weeks to a size of 0.1 mm × 0.1 mm × 0.5 mm in space group $C2$ (a = 264.2 Å, b = 111.5 Å, c = 121.6 Å, and β = 97.4°) and one [(L127Δ-Av2)$_2$−Av1] complex in the asymmetric unit. The nucleotide-bound L127Δ-Av2−Av1 complex was obtained by soaking the crystals in MgATP, prepared with 50 mM ATP and 50 mM $MgCl_2$. The addition of MgATP resulted in a change in space group from $C2$ to $P2_12_12_1$ (a = 110.5 Å, b = 121.5 Å, and c = 264.9 Å) and one complex in the asymmetric unit. The crystals were rapidly frozen on rayon loops in liquid N_2 after soaking in a synthetic mother liquor containing 10% glycerol. During data collection, the crystals were cooled by a continuous nitrogen stream at approximately 100 K. X-ray diffraction data were recorded with a MAR imaging plate detector on beamline 7-1 (λ = 1.08 Å) of the Stanford Synchrotron Radiation Laboratory. The data were processed using DENZO and SCALEPACK (*19*), and statistics are presented in Table 1.

The structure of the nucleotide-free L127Δ-Av2−Av1 complex was determined by molecular replacement with the program AMORE (*20*) using the 2MIN structure of Av1 as a search model. The solution gave an R-factor of 0.39 and a correlation of 0.51 to 4.0 Å resolution. The sites of the L127Δ-Av2 [4Fe-4S] clusters and proximal secondary structure elements were readily distinguishable in the initial electron density maps. These were used for an approximate placement of the Av2 dimers in the initial phasing and construction of masks for 2-fold averaging and solvent flattening. The 2-fold averaging included the noncrystallographic symmetry relationship between the equivalent halves of the complex. Phases were refined and extended from 4.0 to 2.5 Å resolution over 150 cycles of 2-fold averaging and solvent flattening with the density modification algorithm SOLOMON (*21*) with a solvent content of 50%. Detailed model building was performed by fitting of individual amino acid residues to the electron density using the program O (*22*).

The structure was initially refined with the program X-PLOR (*23*) using the protein parameters of Engh and Huber (*24*) and noncrystallographic symmetry restraints. The quality of the model was improved through cycles of model rebuilding, simulated annealing and individual B-factor refinement, and density modification using the data from 20 to 2.2 Å resolution. The CNS program was used for further refinement (*25*), and the model was subjected to several cycles of simulated annealing at 2.2 Å resolution, with a bulk solvent and anisotropic B-factor correction applied. A total of 924 water molecules with B-factors of <52 Å^2 and with geometrically reasonable H-bonds were added, and the noncrystallographic symmetry restraints were removed.

The nucleotide-bound complex (L127Δ-Av2−ATP−Av1) was determined by molecular replacement with the program AMORE (*20*), using data between 8 and 4.15 Å resolution. This model was optimized by rigid-body refinement incorporating the data between 20 and 3.15 Å resolution to give an R-factor of 0.38 and a correlation coefficient of 0.54. A consistent molecular replacement solution was also obtained with the program EMPR (*26*), using data between 15 and 4 Å resolution, to identify a model giving an R-factor of 0.42

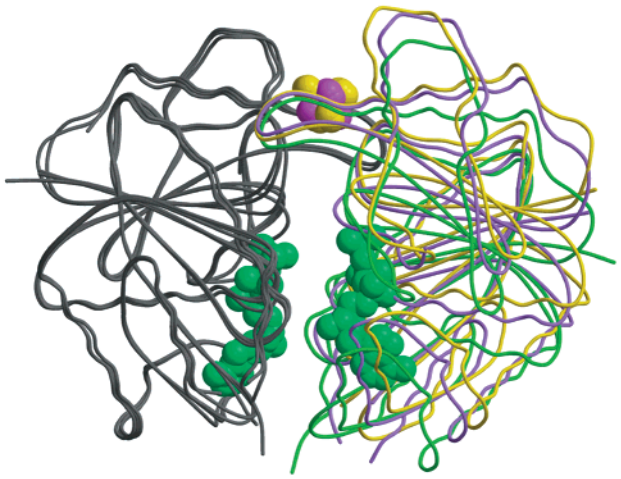

FIGURE 2: Superposition of the peptide backbone for Fe-protein dimers observed in complex with Av1: Av2 in the Av2−ADP·AlF_4^-−Av1 complex (green), L127Δ-Av2 in the L127Δ-Av2−Av1 complex (purple), and L127Δ-Av2 in the L127Δ-Av2−ATP−Av1 complex (gold). For this superposition, the β-sheet residues were used in the Fe-protein subunit of each dimer that interacts with the MoFe-protein α-subunit. The MgATP from the L127Δ-Av2−ATP−Av1 complex is in green, while the nucleotide in the Av2−ADP·AlF_4^-−Av1 complex has been omitted for clarity of presentation.

and a correlation coefficient of 0.60. The molecular replacement phases were improved and gradually extended to 3 Å resolution by histogram matching, solvent flattening (solvent content of 50%), and 2-fold noncrystallographic averaging using the program DM (*27*). The model was refined using the data from 20 to 3 Å resolution in the program CNS where the torsion angle dynamics option and tight noncrystallographic symmetry restraints were applied. During the process of refinement, the noncrystallographic symmetry restraints were loosened for the residues of flexible loop regions and two FeMo-cofactors, two P-clusters, and two [4Fe-4S] clusters were included. Once the model statistics were reasonable, the ATP molecules were built into the electron density. At the final stages of refinement, only one monomer of L127Δ-Av2 at a time was refined while fixing the rest of the structure.

The final models for the structures of the two complexes contain one Av1 molecule with two α-subunits (residues 5−480) and two β-subunits (residues 2−523), two L127Δ-Av2 units with two identical subunits (residues 2−271), two FeMo-cofactors, two P-clusters, and two [4Fe-4S] clusters. The nucleotide-free structure also has 924 water molecules, while the nucleotide-containing structure has four MgATP molecules. The numbering of residues in Av1 is based upon the gene sequences using the designation of α or β for the two different subunits (*28*). The two identical subunits of L127Δ-Av2 are numbered without designation and based upon the Av2 protein sequence (*29*). The refinement statistics are summarized in Table 1.

The Protein Data Bank [PDB (*30*, *31*)] identifiers of the coordinate sets used for the structural comparisons described in this report include 2NIP [*A. vinelandii* Fe-protein (*32*)], 2MIN [*A. vinelandii* MoFe-protein (*17*)], and 1N2C [wild-type *A. vinelandii* nitrogenase complex stabilized with ADP·AlF_4^- (*9*)].

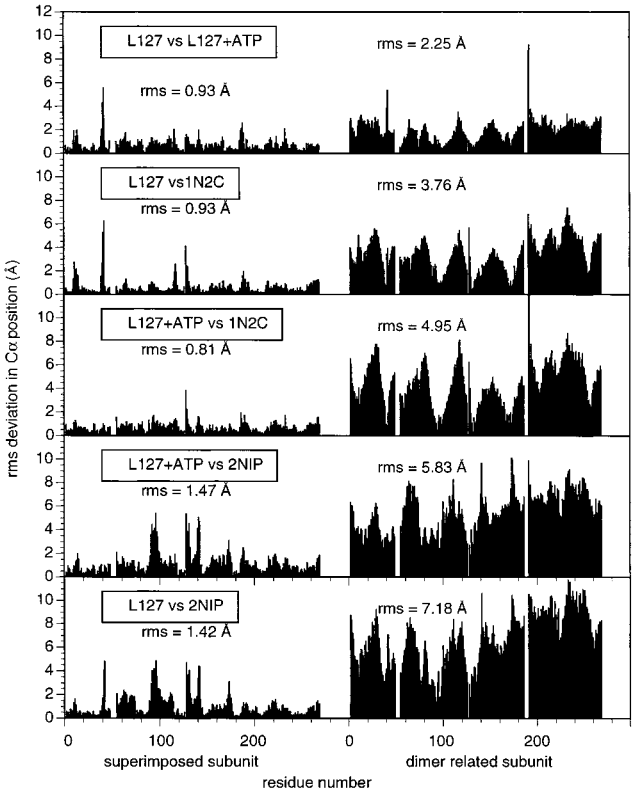

FIGURE 3: Root-mean-square differences in Cα positions between residues in different Fe-protein structures. For this superposition, the β-sheet residues were used in the Fe-protein subunit of each dimer that interacts with the MoFe-protein α-subunit. Comparisons between Cα positions in these subunits are on the left-hand side of the figure (superimposed subunit), while comparisons between Cα positions in the second subunit that was not used in the superposition are on the right-hand side of the figure (dimer related subunit). The rms deviations in Cα positions are indicated. Coordinate sets are identified as L127, L127+ATP, 1N2C, and 2NIP for Fe-proteins in the L127Δ-Av2−Av1, L127Δ-Av2−ATP−Av1, Av2−ADP·AlF_4^-−Av1 (PDB entry 1N2C), and wild-type (uncomplexed) Av2 (PDB entry 2NIP) structures.

RESULTS AND DISCUSSION

Overall Structure. The structure of the tight binding complex between L127Δ-Av2 and Av1, formed in the absence of bound nucleotide, has been determined by molecular replacement and refined at 2.2 Å resolution. As anticipated, the proteins in the complex are in a ratio of two L127Δ-Av2 (γ_2) dimers to one Av1 $\alpha_2\beta_2$ tetramer, and the complex can be viewed as a dimer of two $\alpha\beta\gamma_2$ units, with a molecular 2-fold axis relating the two halves. The L127Δ-Av2 binding site on Av1 is at the interface between the α- and β-subunits near the P-cluster, such that the surface around the [4Fe-4S] cluster of Av2 contacts Av1. In this position, the two γ-subunits in Av2, as well as the homologous α- and β-subunits in Av1, are related by local 2-fold axes; the two axes are nearly parallel (inclined at ∼5.5° to each other) and offset by ∼2 Å at the [4Fe-4S] cluster.

Two features are immediately evident upon examination of the structures (shown in Figure 1 for the L127Δ-Av2−Av1 complex with bound MgATP). First, structural changes observed in the complex, when compared to the isolated wild-type proteins, occur primarily in L127Δ-Av2, with few obvious differences in Av1. Second, the binding mode for L127Δ-Av2 with Av1 is essentially identical to that previ-

Table 2: Av2 Dimer Interactions[a]

Av2−ADP·AlF_4^-	L127Δ-Av2	L127Δ-Av2−ATP	Av2[b]
R46(Nη2)−E265(Oϵ1)	**R46(Nη2)−E265(Oϵ1)**		
G94(N)−V130(O)	**G94(N)−V130(O)**	**G94(N)−V130(O)**	**G94(N)−V131(O)**
G94(O)−Y171(OH)	**G94(O)−Y171(OH)**	**G94(O)−Y171(OH)**	
	G96(O)−G133(N)	**G96(O)−G133(N)**	G96(O)−G133(N)
A98(N)−V131(O)	A98(N)−V131(O)		
D129(Oδ2)−D129(N)			
E154(Oϵ2)−R213(Nη2)			
N188(O)−N215(Nδ2)			
			R223(O)−G283(N)
			R223(Nη1)−K284(O)
			R224(Nη1)−E277(Oϵ2)
			Y230(O)−A286(N)
E265(Oϵ2)−R46(Nϵ)	E265(Oϵ2)−R46(Nϵ)		
			I281(O)−R223(Nη1)

[a] Hydrogen bond and ionic interactions less than 3.3 Å in length at the subunit−subunit interface of the Av2 dimer in the indicated structures are listed. The symmetric interactions are shown in bold. Residues on the left and right side of each pair are in the Fe-protein subunit that interacts primarily with the α- and β-subunits of the MoFe-protein, respectively. [b] PDB entry 2NIP.

ously found for the native nitrogenase proteins stabilized by MgADP·AlF_4^-. Although the similarities in the general binding interactions might have been anticipated, there was no imperative that they be so nearly identical to the native protein complex. The Av1 structures in both complexes are remarkably similar to that of free Av1 (0.3 Å rms differences in Cα positions), with the largest changes occurring in the areas of Av1 interacting with the Fe-protein. Most importantly, no major structural changes are evident around the FeMo-cofactor, while the P-cluster resembles that previously characterized as the P^{OX} oxidation state (*17*). As observed for the MgADP·AlF_4^- complex, striking structural changes take place in the Fe-protein component, at least in comparison to the autonomous, nucleotide-free, wild-type protein. The conformational changes are seen as the reorientation of the subunits leading to a more compact and closed interface between them. As a consequence, the bridging [4Fe-4S] cluster has been thrust ∼4 Å toward the MoFe-protein surface to a center−center separation from the P-cluster of 17.9 Å (edge-to-edge distance ∼ 14 Å). For comparison, the centers of the two clusters are separated by 17.4 Å in the ADP·AlF_4^--stabilized complex. The oxidation state of the Fe-protein [4Fe-4S] cluster in this complex cannot be established through these crystallographic studies.

The structure of the complex between L127Δ-Av2 and Av1 with MgATP bound is shown in Figure 1. As with the structures of the two other complexes, the significant conformational changes reside in the Fe-protein component. Since the material used for this structural analysis was obtained by soaking crystals of the nucleotide-free complex with MgATP, the nucleotide binding sites in the L127Δ-Av2 complex must be accessible for binding by exogenously added nucleotides. The large-scale orientations of the L127Δ-Av2 subunits with nucleotide are similar to those without nucleotide, although the subunit interface is not as closely packed as in the nucleotide-free complex. A more detailed description and comparison of the Av2 components follows.

Global Conformational Changes in the Fe-Protein Component. Four states of Av2 are now available for structural comparison: wild-type, nucleotide-free, uncomplexed Av2; wild-type, ADP·AlF_4^--bound Av2 in complex with Av1; nucleotide-free, L127Δ-Av2 in complex with Av1; and MgATP-bound L127Δ-Av2 in complex with Av1. The structural relationships between the three complex-bound forms of Fe-protein are illustrated in Figure 2 which was generated by superimposing Cα atoms in the structurally conserved, core β-sheets in the Fe-protein subunit in each complex most closely associated with the α-subunit of the MoFe-protein. Structural differences between native, nucleotide-free Av2 and the complex-bound L127Δ-Av2 (with or without nucleotide) include both the relative orientation between the two monomers in the dimer and local changes in tertiary structure, particularly in structural elements outside the β-sheet (Figure 3). In the complex, the L127Δ-Av2 monomers, acting as rigid bodies, have rotated toward each other, resulting in a new set of interactions at the dimer interface that are summarized in Table 2. The four Av2 structures (three in complexes and the uncomplexed wild-type Av2) appear to exhibit a gradation of "closure" between the subunits, with native Av2 the most open and native Av2-bound ADP·AlF_4^- in complex with Av1 the most closed. Using one subunit as a reference, then relative to the free Av2 structure, the second subunit in the L127Δ-Av2−ATP−Av1, the L127Δ-Av2−Av1, and the Av2−ADP·AlF_4^-−Av1 complexes exhibits a rigid body rotation of ∼18°, 22°, and 25°, respectively, about an axis positioned approximately along the subunit−subunit interface and normal to the Fe-protein 2-fold axis. Consequently, the two L127Δ-Av2 structures are intermediate between the structures of native Av2 in the unliganded and ADP·AlF_4^--stabilized complex forms. Most interestingly, L127Δ-Av2 in complex with bound nucleotide is more open than the nucleotide-free form; that is, binding of ATP by L127Δ-Av2 leads to a somewhat more open conformation in complex with Av1, while binding of ADP·AlF_4^- by wild-type Av2 in complex with Av1 leads to a decidedly more closed structure.

Component Protein Interface. The closure of the Fe-protein dimer interface observed in all three complexes allows the formation of stabilizing interactions across the component protein interface, i.e., the interface between Av2 and Av1. These interactions are extensive and bury ∼3600 $Å^2$ in surface area at each Av1−Av2 interface (corresponding to ∼900 $Å^2$ of surface area buried for each α-subunit, β-subunit, and two Fe-protein subunits participating in a given interface). The large contact surface at the Av1−Av2 interface is achieved by the conformational changes in Av2 forms compared to the native nucleotide-free Av2; without the changes, most of the hydrogen bonds and electrostatic

Table 3: Av2−Av1 Intermolecular Contacts[a]

Av2 residue−Av1 residue		
L127Δ-Av2−Av1	L127Δ-Av2−ATP−Av1	Av2−ADP·AlF_4^-−Av1
Monomer Associated with a MoFe α-Subunit		
C97(N)−Vβ124(O)	C97(N)−Vβ124(O)	C97(N)−Vβ124(O)
R100(Nη1)−Gα157(O)	R100(Nη1)−Gα157(O)	R100(Nη1)−Gα157(O)
		R100(Nη2)−Eα184(Oε1)
R100(Nη2)−Eβ120(Oε2)	R100(Nη2)−Eβ120(Oε2)	
T104(Oγ)−Eβ120(Oε2)	T104(Oγ)−Eβ120(Oε2)	T104(Oγ)−Eβ120(Oε2)
		G133(N)−Iα159(O)
R140(Nη2)−Gα160(O)		
E141(Oε1)−Kα168(Nζ)		
Monomer Associated with a MoFe β-Subunit		
A62(O)−Kα121(Nζ)		
C97(N)−Vα124(O)	C97(N)−Vα124(O)	C97(N)−Vα124(O)
R100(Nε, Nη2)−Eα120(Oε2)	R100(Nε, Nη2)−Eα120(Oε2)	R100(Nε, Nη2)−Eα120(Oε2)
R100(Nη1)−Eβ156(Oε1, O)	R100(Nη1)−Eβ156(Oε1)	R100(Nη1)−Eβ156(Oε1)
T104(Oγ)−Eα120(Oε2)	T104(Oγ)−Eα120(Oε2)	T104(Oγ)−Eα120(Oε2)
G133(N)−Iβ158(O)		G133(N)−Iβ158(O)
	E111(O)−Kβ303(Nζ)	
R140(Nη2)−Gβ159(O)		
		K170(O)−Nβ168(Nδ2)

[a] Hydrogen bond and ionic interactions less than 3.3 Å in length are shown.

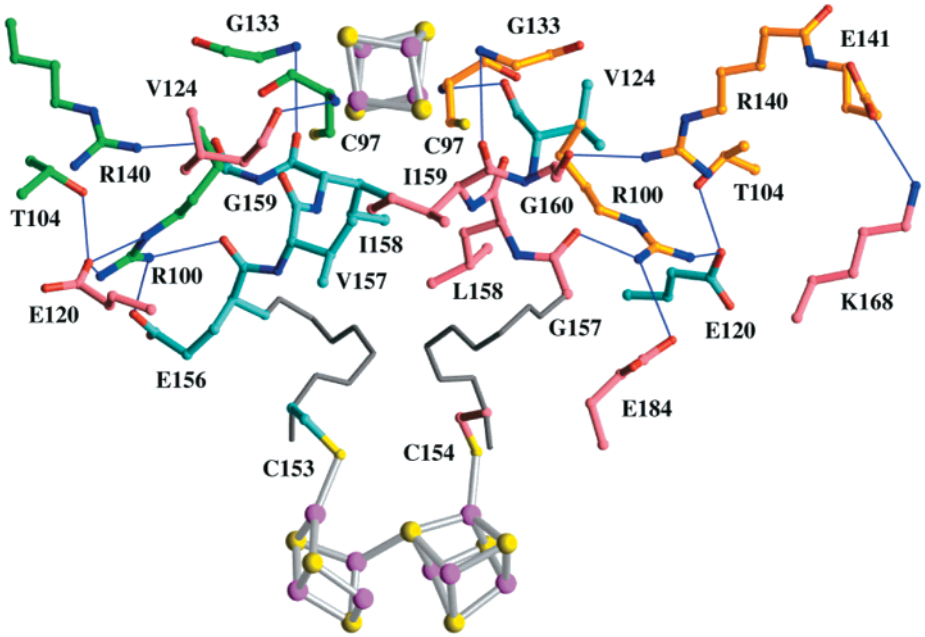

FIGURE 4: Interface between Av2 and Av1 in the L127Δ-Av2−Av1 complex. Residues from the MoFe-protein α-subunit are shown with red backbones, the β-subunit with light-blue backbones, and the individual subunits of each Fe-protein with gold and green backbones. Atoms are colored according to the scheme described in the legend of Figure 1.

interactions in the interface would not be possible. A summary of the contacts at the Av1−Av2 interface for the three complexes is provided in Table 3. A web of polar interactions involving salt bridges and hydrogen bonds, including some involving water molecules, connects the component proteins. As illustrated in Figure 4, both oppositely charged pairs of side chains, as well as like-charged pairs, are juxtaposed at the interface between the component proteins, indicating that the energetic balance of these electrostatic interactions is delicately poised. The complexity of the ionic interactions at this interface must contribute to the ionic strength sensitivity of the nitrogenase reaction (*33*).

The overwhelming conclusion from a detailed comparison is that most of the specific Av2−Av1 interface interactions described for the ADP·AlF_4^--stabilized Av2−Av1 complex (*9*) are conserved in the L127Δ-Av2−Av1 complexes. The level of congruence includes the near superposition of the Av2 [4Fe-4S] clusters in the three complexes. At least to this degree, the L127Δ-Av2−Av1 structures appear to represent electron transfer competent complexes equivalent to that in the Av2−ADP·AlF_4^-−Av1 complex (Figure 5), consistent with observations that interprotein electron transfer can be observed in the L127Δ-Av2−Av1 complex (*15*). Given that L127Δ-Av2 and wild-type Av2−ADP·AlF_4^- in the complexes differ in the regions away from their interface with Av1 (see below), it appears that Av1 is a dominant template for stable complex formation; albeit, other transient complexes must be possible such as that during chemical cross-linking between components by carbodiimides (*34*, *35*).

Nucleotide Binding to the L127Δ-Av2−Av1 Complex. The ATP binding site in the L127Δ-Av2−Av1 complex is along the same surface of the Fe-protein subunit interface observed

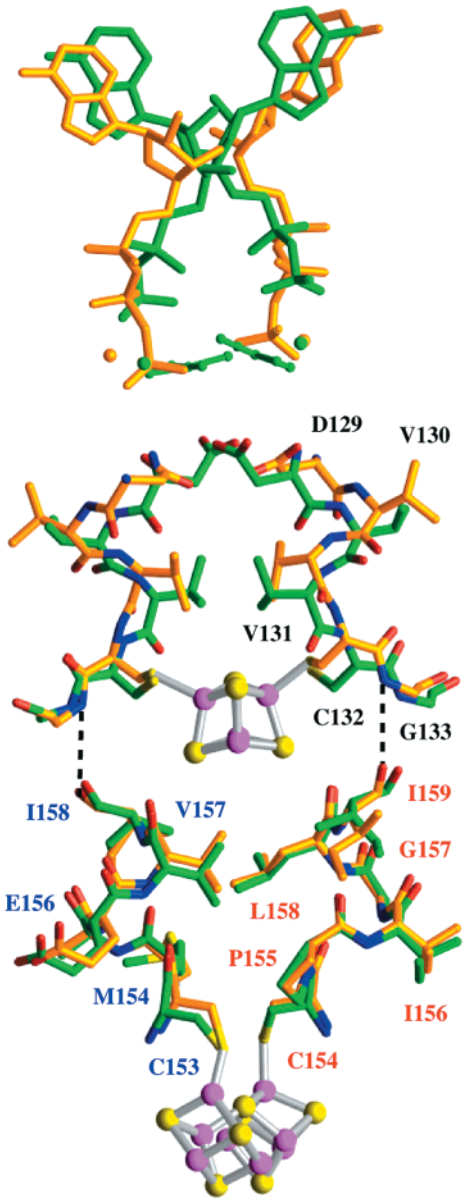

FIGURE 5: Comparison of nucleotide binding site and electron transfer pathways in the L127Δ-Av2−ATP−Av1 (gold backbone) and Av2−MgADP·AlF_4^-−Av1 (green backbone) complexes, achieved by superposition of the Cα positions of the MoFe-protein α- and β-subunits. MgATP and MgADP·AlF_4^- are colored gold and green, respectively.

for the binding of ADP·AlF_4^-. Although low levels of ATP hydrolysis by this complex have been reported,[1] the electron density maps clearly show that the bound nucleotide is ATP. There are differences in the protein−nucleotide interactions observed in the L127Δ-Av2−ATP−Av1 and Av2−ADP·AlF_4^-−Av1 complexes, which may be relevant to the greatly reduced rate of ATP hydrolysis in the former relative to that in the latter complex. As shown in Figure 6, the ATP conformers in two subunits of L127Δ-Av2 are different, especially in terms of the orientation of the two adenine rings which are rotated ~90° to each other; in contrast, the adenine rings in the ADP·AlF_4^--stabilized nitrogenase complex are oriented virtually identically with respect to each Av2 subunit. Examination of the rms deviations as a function of residue number for the Av2 forms in complex with Av1 (Figure 3) indicates that regions with high deviations between

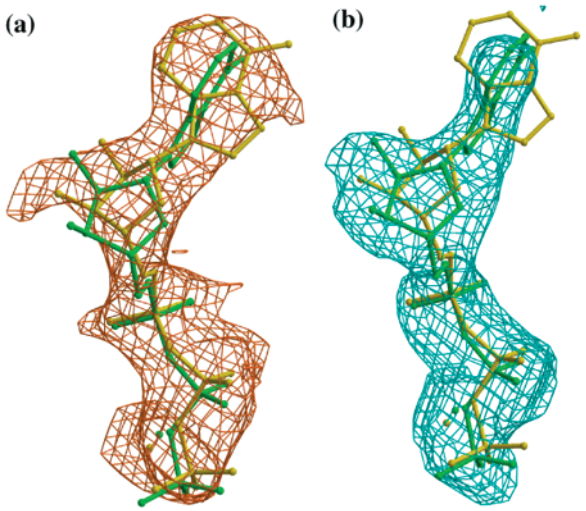

FIGURE 6: Comparison of the two nucleotide binding modes in the L127Δ-Av2−ATP−Av1 complex. (a) MgATP (yellow) associated with the L127Δ-Av2 subunit interacting with the MoFe-protein α-subunit. The difference electron density map shown in brown was generated from a refined omit map calculated for this residue. For direct comparison of the different modes for MgATP binding to the two Fe-protein subunits, the second MgATP (green) bound to the other Fe-protein subunit is illustrated, following application of the appropriate transformations to superimpose the two subunits. (b) Equivalent view of the MgATP (green) bound to the L127Δ-Av2 subunit that interacts with the MoFe-protein β-subunit, with the omit refine density contoured in cyan. These superpositions illustrate that while the phosphate groups of the two nucleotides bound per Fe-protein dimer interact similarly with each subunit, the adenine rings are approximately orthogonal and hence interact with each Fe-protein subunit in distinctive manners (see Figure 7).

structures generally correspond to the binding sites for nucleotide, while the β-sheet residues form a structurally conserved core that effectively behaves as a rigid unit. With the exception of the 50s region, the greatest differences include residues that have intimate interactions with nucleotide, in particular the P-loop, switch I, switch II, and the adenine ring. It is noteworthy that many of the interactions with nucleotide observed for the Av2−ADP·AlF_4^- species that are missing or different in the L127Δ-Av2−ATP species appear to be critical for the nucleotide hydrolysis mechanism. The most obvious of these residues are Lys 10, Lys 15, Lys 41, Gly 128, and Asp 129. Details of the nucleotide interactions in the two complexes are summarized in Table 4 and Figure 7.

Leu 127 is part of the so-called switch II region, first identified in *ras* as having the largest conformational differences between the GTP and GDP states. Also in the sequence are residues directly connected to the nucleotide hydrolysis process. In Av2, this sequence extends to Cys 132, which supplies two (one from each subunit) of the four ligands to the [4Fe-4S] cluster and which may serve to anchor one end of the switch region. As shown in Figure 8, upon deletion of Leu 127, the peptide backbone is altered such that the next two residues, Gly 128 and Asp 129, cannot have the same position as in wild-type Av2; both residues are central to the nucleotide interactions and hydrolysis. These conformational alterations associated with the deletion of Leu 127 are independent of whether nucleotide is present and, significantly, are not compensated when nucleotide is bound. The first uncompensated change is in the positioning

Table 4: Interactions between Av2 and Nucleotides[a]

	L127Δ-Av2−ATP		
	monomer 1[b]	monomer 2[b]	Av2−ADP·AlF_4^-
phosphate			
O1A	T17(N, Oγ)	T17(N, Oγ) S16(Oγ)	T17(N, Oγ)
O2A			K10′(Nζ)
O3A			G14(N)
O1B	K15(N) S16(N)	K15(N) S16(N)	K10′(Nζ)
O2B	G12(N)	G12(N)	S16(N, Oγ) K15(N)
O3B			G12(N) G14(N) K15(Nζ)
O1G	K15(Nξ)	K15(Nζ)	
O2G	K10′(Nζ) K41(Nζ)		
F1			G128(N) K15(Nζ)
F2			K10′(Nζ) K41(Nζ)
F3			G12(N)
F4			K10′(Nζ) S16(Oγ)
sugar			
O2*		E221(Oϵ1)	
O3*	E221(Oϵ1, Oϵ2)		E221(Oϵ1)
base			
N1			D214(N)
N6	P212(O)	Q236(Oϵ1)	P212(O)
N7	N185(Nδ2)		N185(Nδ2)

[a] Hydrogen bond and ionic interactions less than 3.3 Å in length are shown. [b] Monomer 1 is the Fe-protein subunit associated with the MoFe α-subunit and monomer 2 that associated with the MoFe β-subunit.

of the amide nitrogen of Gly 128, which serves as a hydrogen bond donor to one of the fluorides of AlF_4^-. This hydrogen bond interaction to the equivalent of the departing phosphate is likely essential for stabilizing the transition state for ATP hydrolysis. To effect this interaction, the peptide backbone around Gly 128 moves ∼ 4 Å in the ADP·AlF_4^--stabilized complex, which cannot be attained when the peptide chain is shortened by the deletion of Leu 127. Indeed, the Gly 128 NH group points away from the nucleotide γ-phosphate in the ATP-bound form of the L127Δ-Av2 complex structure, and hence is unable to hydrogen bond with this group. The second major change in this sequence is Asp 129, whose side chain carboxyl group hydrogen bonds and directs the putative attacking water on the terminal phosphate of the ATP. This residue in the native complex is notable because it is directed across the Av2 subunit interface. With the deletion of Leu 127, the Asp 129 side chain no longer can reach across the interface, nor is it able to reach the nucleotide bound in the same subunit, thereby diminishing the catalytic efficiency of this process.

Following these two catalytically crucial residues are Val 130 and Val 131 that were identified in the Av2−ADP·AlF_4^-−Av1 structure as having undergone reorganization in the region immediately below the [4Fe-4S] cluster. For this reason, we previously suggested that the valines might be part of the switching process leading to the larger conformational changes in Av2 (*9*). Interestingly, these two valines in L127Δ-Av2 appear to have substantially the same structure as those in the Av2−ADP·AlF_4^-−Av1 complex. This suggests that the effects of the deletion have been partially mitigated at a distance of three and four residues following the deletion, thereby accommodating the conformational changes required for binding to Av1.

In addition to the more localized changes, conformational rearrangements in L127Δ-Av2 are propagated in regions away from the deletion site. For example, the backbone position of Lys 10 in the P-loop region is shifted by ∼3 Å from the location observed in the ADP·AlF_4^--stabilized nitrogenase complex (Figure 3). In the latter structure, the side chain of Lys 10 mediates the catalytically critical stabilization of the developing negative charge on the bridging oxygen of the γ−β-phosphates of ATP during nucleotide hydrolysis. As with Asp 129, Lys 10 exerts its action across the Av2 subunit interface to the ATP bound on the opposite subunit. In this way, Lys 10 also contributes to the stability of the intersubunit bonding. Another significant intersubunit bond that is found in the Av2−ADP·AlF_4^-−Av1 complex, but not in the L127Δ-Av2−ATP−Av1 complex, involves Glu 154 of one Av2 subunit and Arg 213 of the other, along with the symmetry-related interaction. These residues are at the opposite side of the Av2 molecule from the cluster and switch II region containing the Leu 127 deletion, and the residues appear to help stabilize the closure of the other end of the nucleotide binding site, at the adenine base. Not withstanding that this region is ∼20 Å from the site of the deletion, in the L127Δ-Av2−ATP−Av1 complex these two residues are distant from each other and do not form a salt bond, and their side chains point in different directions in the two complexes.

These structural studies start to address how the L127Δ mutation leads to stable complex formation between the Fe-protein and the MoFe-protein in the absence of nucleotide. Without any tertiary structure rearrangements, if the subunits of the isolated wild-type Av2 are computationally docked onto the subunits of the Fe-protein in the L127Δ-Av2−Av1 complex, significant steric overlap exists between residues 93 and 94 of one subunit and residues 131 and 133 of the other subunit. Consequently, one or more of these regions must rearrange upon going to the quaternary structure seen for the Fe-protein in the MoFe-protein complex. With wild-type Av2, the conformational change of the switch II region appears to be coupled to the formation of a hydrogen bond between the Gly 128 NH and the γ-phosphate of ATP, which then leads to the repositioning of Asp 129, Val 130, Val 131, and Cys 132. The change in these residues is coupled to a shift in cluster position. The deletion of Leu 127 apparently short-circuits this process by requiring a different loop conformation to complete the connection between residues 126 and 133 which are superimposable in the free and complex forms; this conformation exhibits similar positions for residues 130−132 that are coupled to the cluster rearrangement, but the shorter loop cannot place Gly 128 and Asp 129 in position for nucleotide hydrolysis. Presumably, the deletion of Leu 127 is not unique in this ability, and it would also be of interest to see the consequences of the homologous mutation in G-proteins.

Implications for MgATP Hydrolysis and Electron Transfer. The detailed differences in nucleotide binding between the L127Δ-Av2−Av1 and Av2−ADP·AlF_4^-−Av1 complexes indicate that the mechanism of nucleotide hydrolysis by L127Δ-Av2 must be different than that proposed for the wild-type protein (*9*). Many of the interactions between the

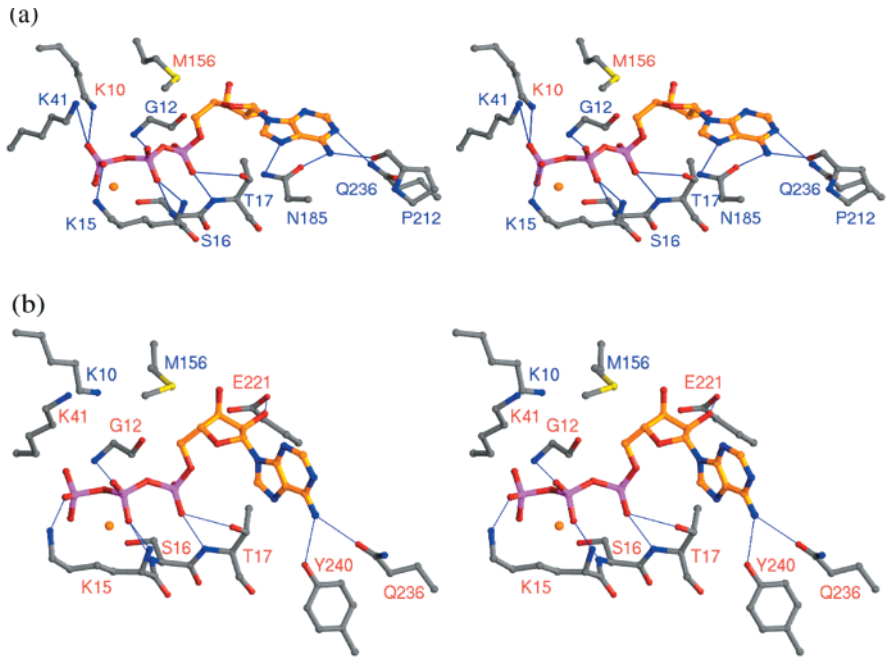

FIGURE 7: Stereoview of the MgATP binding sites in the L127Δ-Av2−ATP−Av1 complex. (a) Nucleotide binding to the L127Δ-Av2 subunit that interacts with the MoFe-protein α-subunit. (b) Nucleotide binding to the L127Δ-Av2 subunit that interacts with the MoFe-protein β-subunit. Atoms are colored according to the scheme described in the legend of Figure 1.

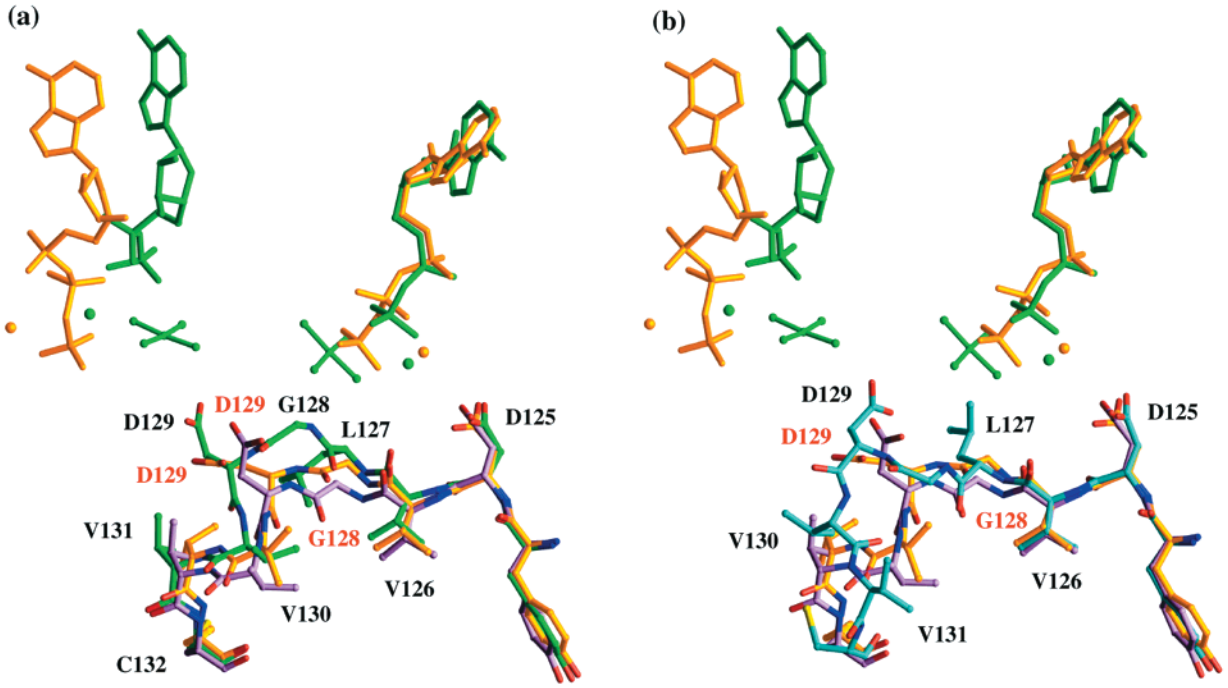

FIGURE 8: Superposition of the switch II region of the Fe-proteins in the L127Δ-Av2−Av1 (purple backbone) and L127Δ-Av2−ATP−Av1 (gold backbone) complexes with (a) the Fe-protein in the Av2−ADP·AlF_4^-−Av1 complex (green backbone) and (b) wild-type, nucleotide-free Av2 in the absence of Av1 (cyan backbone, PDB entry 2NIP). MgATP and MgADP·AlF_4^- are colored gold and green, respectively. The displayed Fe-protein subunits were superimposed using the Cα positions of the β-sheet residues.

nucleotide and the protein seen in the ADP·AlF_4^--stabilized complex are missing in the L127Δ-Av2 complex, yet these interactions are not replaced by alternate interactions that might allow for efficient catalysis. Because the process of electron transfer is intimately tied to nucleotide hydrolysis, the deletion of Leu 127 must alter or prevent some conformational states in the multiple steps of electron transfer, thus blocking complete cycling and turnover of the active complexes. These distinctions exist even though the metallocenters have very similar positions in both the ADP·AlF_4^-- and L127Δ-Av2-stabilized complexes. For example, the reduction of Av1 by Av2 involves the formation of a two-protein complex with ATP, ATP hydrolysis, electron transfer, phosphate release, and dissociation of the protein complex. The stability of the transient complex of the Fe-protein and the MoFe-protein must play an important role during electron transfer (*1*, *10*). The L127Δ-Av2−Av1 complex, without the ability to efficiently turn over nucleotide, appears to be frozen in a stage of tight binding and alignment of the redox centers approaching electron transfer.

The properties of L127Δ-Av2 raise important questions concerning the mechanistic role of dissociation of the nitrogenase complex. Kinetic analyses of nitrogenase have identified dissociation of the Av1−Av2 complex as the rate-determining step (*36*). The requirement for dissociation of the nitrogenase complex has been assumed to allow re-reduction of the Fe-protein and exchange of MgADP for ATP. Biochemical studies on this and other systems have shown that the Fe-protein complexed to the MoFe-protein can be reduced by the physiological reductant flavodoxin (*37*, *38*), although apparently not by dithionite which is used in many kinetic studies. Although the Fe-protein dimer is significantly more closed in the L127Δ-Av2−Av1 complex than observed in free wild-type Av2, this study demonstrates that the nucleotide site is accessible to binding by added nucleotide, reinforcing earlier observations from solution studies (*37*, *39*). While it has not been determined whether nucleotide binding to the complex is sufficiently fast for it to be kinetically significant, clearly, dissociation is not obligatory for this process to occur. Consequently, the requirement and role for complex dissociation in the nitrogenase mechanism may need to be reconsidered in view of these observations. As for many other enzymes, careful analyses of the properties of mutant nitrogenases can provide a powerful approach for probing the structure and mechanism of this complex system.

REFERENCES

1. Howard, J. B., and Rees, D. C. (1994) *Annu. Rev. Biochem. 63*, 235−264.
2. Burgess, B. K., and Lowe, D. J. (1996) *Chem. Rev. 96*, 2983−3011.
3. Seefeldt, L. C., and Dean, D. R. (1997) *Acc. Chem. Res. 30*, 260−266.
4. Smith, B. E. (1999) *Adv. Inorg. Chem. 47*, 159−218.
5. Rees, D. C., and Howard, J. B. (2000) *Curr. Opin. Chem. Biol. 4*, 559−566.
6. Kjeldgaard, M., Nyborg, J., and Clark, B. F. C. (1996) *FASEB J. 10*, 1347−1368.
7. Sprang, S. R. (1997) *Annu. Rev. Biochem. 66*, 639−678.
8. Miller, R. W., Eady, R. R., Gormal, C., Fairhurst, S. A., and Smith, B. E. (1998) *Biochem. J. 334*, 601−607.
9. Schindelin, H., Kisker, C., Schlessman, J. L., Howard, J. B., and Rees, D. C. (1997) *Nature 387*, 370−376.
10. Rees, D. C., and Howard, J. B. (1999) *J. Mol. Biol. 293*, 343−350.
11. Wittinghofer, A. (1997) *Curr. Biol. 7*, R682−R685.
12. Ryle, M., and Seefeldt, L. C. (1996) *Biochemistry 35*, 4766−4775.
13. Lanzilotta, W. N., Fisher, K., and Seefeldt, L. C. (1996) *Biochemistry 35*, 7188−7196.
14. Wolle, D., Dean, D. R., and Howard, J. B. (1992) *Science 258*, 992−995.
15. Lanzilotta, W. N., and Seefeldt, L. C. (1996) *Biochemistry 35*, 16770−16776.
16. Seefeldt, L. C. (1994) *Protein Sci. 3*, 2073−2081.
17. Peters, J. W., Stowell, M. H. B., Soltis, S. M., Finnegan, M. G., Johnson, M. K., and Rees, D. C. (1997) *Biochemistry 36*, 1181−1187.
18. Georgiadis, M. M., Komiya, H., Chakrabarti, P., Woo, D., Kornuc, J. J., and Rees, D. C. (1992) *Science 257*, 1653−1659.
19. Otwinowski, Z., and Minor, W. (1997) *Methods Enzymol. 276*, 307−326.
20. Navaza, J. (1994) *Acta Crystallogr. A50*, 157−163.
21. Abrahams, J. P., and Leslie, A. (1996) *Acta Crystallogr. D52*, 30−42.
22. Jones, T. A., Zhou, J. Y., Cowan, S. W., and Kjeldgaard, M. (1991) *Acta Crystallogr. A47*, 110−119.
23. Brünger, A. T. (1992) *X-PLOR version 3.1: A system for X-ray crystallography and NMR*, Yale University Press, New Haven, CT.
24. Engh, R. A., and Huber, R. (1991) *Acta Crystallogr. A47*, 392−400.
25. Brunger, A., Adams, P., Clore, G., DeLano, W., Gros, P., Grosse-Kunstleve, R., Jiang, J., Kuszewski, J., Nilges, M., Pannu, N., Read, R., Rice, L., Simonson, T., and Warren, G. (1998) *Acta Crystallogr. D54*, 905−921.
26. Kissinger, C., Gehlhaar, D., and Fogel, D. (1999) *Acta Crystallogr. D55*, 484−491.
27. Cowtan, K. D., and Main, P. (1996) *Acta Crystallogr. D52*, 43−48.
28. Brigle, K. E., Newton, W. E., and Dean, D. R. (1985) *Gene 37*, 37−44.
29. Hausinger, R. P., and Howard, J. B. (1982) *J. Biol. Chem. 257*, 2483−2490.
30. Sussman, J., Lin, D., Jiang, J., Manning, N., Prilusky, J., Ritter, O., and Abola, E. (1998) *Acta Crystallogr. D54*, 1078−1084.
31. Berman, H. M., Westbrook, J., Feng, Z., Gilliland, G., Bhat, T. N., Weissig, H., Shindyalov, I. N., and Bourne, P. E. (2000) *Nucleic Acids Res. 28*, 235−242.
32. Schlessman, J. L., Woo, D., Joshua-Tor, L., Howard, J. B., and Rees, D. C. (1998) *J. Mol. Biol. 280*, 669−685.
33. Deits, T. L., and Howard, J. B. (1990) *J. Biol. Chem. 265*, 3859−3867.
34. Willing, A., and Howard, J. B. (1990) *J. Biol. Chem. 265*, 6596−6599.
35. Willing, A. H., Georgiadis, M. M., Rees, D. C., and Howard, J. B. (1989) *J. Biol. Chem. 264*, 8499−8503.
36. Thorneley, R. N. F., and Lowe, D. J. (1985) in *Molybdenum Enzymes* (Spiro, T. G., Ed.) pp 221−284, John Wiley & Sons, New York.
37. Duyvis, M. G., Wassink, H., and Haaker, H. (1998) *Biochemistry 37*, 17345−17354.
38. Lanzilotta, W. N., and Seefeldt, L. C. (1997) *Biochemistry 36*, 12976−12983.
39. Larsen, C., Christensen, S., and Watt, G. D. (1995) *Arch. Biochem. Biophys. 323*, 215−222.
40. Laskowski, R. A., McArthur, M. W., Moss, D. S., and Thornton, J. M. (1993) *J. Appl. Crystallogr. 26*, 283−291.
41. Carson, M. (1991) *J. Appl. Crystallogr. 24*, 958−961.
42. Kraulis, P. J. (1991) *J. Appl. Crystallogr. 24*, 946−950.
43. Merritt, E. A., and Murphy, M. E. P. (1994) *Acta Crystallogr. D50*, 869−873.

BI001645E